2013•2014
FACULTEIT GENEESKUNDE EN LEVENSWETENSCHAPPEN
*master in de biomedische wetenschappen*

# Masterproef

## Array formatting of the heat-transfer method (HTM) for the detection of small organic molecules by molecularly imprinted polymers

Promotor :
Prof. dr. Patrick WAGNER

Copromotor :
dr. Marloes PEETERS


Gideon Wackers


*Proefschrift ingediend tot het behalen van de graad van master in de biomedische wetenschappen*


De transnationale Universiteit Limburg is een uniek samenwerkingsverband van twee universiteiten in twee landen: de Universiteit Hasselt en Maastricht University.

universiteit hasselt
KNOWLEDGE IN ACTION

Universiteit Hasselt | Campus Hasselt | Martelarenlaan 42 | BE-3500 Hasselt
Universiteit Hasselt | Campus Diepenbeek | Agoralaan Gebouw D | BE-3590 Diepenbeek

universiteit hasselt | Maastricht University

2013•2014
FACULTEIT GENEESKUNDE EN LEVENSWETENSCHAPPEN
*master in de biomedische wetenschappen*

# Masterproef

## Array formatting of the heat-transfer method (HTM) for the detection of small organic molecules by molecularly imprinted polymers


Promotor :
Prof. dr. Patrick WAGNER

Copromotor :
dr. Marloes PEETERS



Gideon Wackers


*Proefschrift ingediend tot het behalen van de graad van master in de biomedische wetenschappen*

universiteit hasselt | Maastricht University

# Table of Contents

# List of Symbols and Abbreviations

| | |
|---|---|
| **CNC** | computer numerical control |
| **ELISA** | enzyme-linked immunosorbent assay |
| **HPLC** | high-performance liquid chromatography |
| **IBS** | irritable bowel syndrome |
| **IDE** | interdigitated electrodes |
| **LOD** | limit of detection |
| **MIP** | molecularly imprinted polymer |
| **NIP** | non-imprinted polymer |
| **PBS** | phosphate buffered saline |
| **PDMS** | polydimethylsiloxane |
| **PID** | proportional-integral-derivative (controller) |
| $\mathbf{R_{th}}$ | heat transfer resistance |

# Preface

The internship at IMO, and especially the time I spent with the members of the BIOSensor group, felt to me like the proverbial “cherry on the cake” of my academic career. I have always enjoyed my time as a bachelor and master student at both Maastricht University and UHasselt, but during my internship I lost that feeling of “being a student”. For this I want to thank the people of the IMO and especially the BIOSsensor group.

To Patrick,
You played a big role in my choice for the Bioelectronics and Nanotechnolgy master, the course you gave at the University of Maastricht about bioelectronics was my favorite during the three years of my bachelor. Within a few days I was sold, I knew that this was something I wanted to know more about, so you can imagine my happiness when you told me about the BEN master. Thank you for all the lectures, time and trust.

To Marloes,
I would like to thank you, for all the time you spent helping me with my experiments and giving feedback on the things I wrote. And of course, let’s not forget the chances you gave me, especially allowing me to write an article for Sensors, this meant a great deal to me. I enjoyed my time as your student and it might sound cheesy, but I could not have wished for a better supervisor. Thank you very much for the awesome internship.

To the remaining members of the BIOS group,
The members of the BIOSensor group and a few people from other groups made my time at the IMO a memorable experience. Even though you all deserve a dedicated paragraph, I am going to keep it short. Bart, Thijs, Evelien, Kathia, Andreas, Patricia, Kasper, Matthias, Mohammed, Mehran, Yassin and Karolien, you all made me feel welcome and I enjoyed the casual chatting, “hobby hours” at the lab and countless card games a lot. So I would like to thank you all for the great time at the IMO and I don’t think there is a better group of people to have around you during an internship than the members of the BIOS group.

I also need to thank some students,
For starters; all the (slightly crazy) Brazilians and Michael for the great time while they were here. And of course my fellow student Peter, with whom I’m currently sharing a desk, was also of great help during the internship. I want to thank all of you for the great time, and the blood, that quite a few of you donated to my experiments.

To the reader,
I hope you enjoy reading my thesis, it involved some of my blood and that of people who happened to walk by during those experiments. Sometimes I’ve even been sweating a little bit during some important experiments but luckily we could leave the tears out. So I hope that my research was worth all the not-so-proverbial “blood, sweat and ~~tears~~” that were put into it.

Gideon

# Summary

In this work we present the first steps towards a molecularly imprinted polymer (MIP) based biomimetic sensor array for the detection of small organic molecules via the heat-transfer method (HTM). The heat-transfer method relies on the change in thermal resistance upon binding of the target molecule to the MIP-type receptor. This technique can be implemented at low-cost because it requires not more than two thermocouples in combination with a proportional-integral-derivative (PID)-controlled heat source. A new flow-through sensor cell is developed which is segmented into four quadrants with a volume of 2.5 µL each, allowing four measurements to be done simultaneously, on a single substrate. It also becomes possible to correct for non-specific binding since one of the channels can be functionalized with a non-imprinted polymer (NIP) which serves as a negative control. The quadrants were functionalized with different MIPs designed for serotonin, histamine and L-nicotine. To produce an adhesion layer MDMO-PPV was spin coated onto aluminum substrates after which the MIP particles were functionalized onto the surface.

Serotonin and histamine are both neurotransmitters indispensable for various physiological processes in the human body. Besides their physiological function, serotonin and histamine are biomarkers for diseases such as irritable bowel syndrome (IBS). As serotonin and histamine have similar functional groups but differ in size, L-nicotine was chosen because of its dimensions, which are similar to those of histamine. When combined, these small organic molecules have similarities in both size and functional groups which demonstrates the specificity of the MIPs. After verification experiments, two arrays capable of discriminating between histamine and serotonin, or histamine and L-nicotine, were analyzed and proven to be successful. As a proof of principle experiment a new flow cell, with a capillary pump for blood, was designed. Incorporated are two sensor surfaces for a MIP and a NIP. Spiked whole blood was added to this flow cell resulting in a detectable change in $R_{th.}$

With the improved array format flow cell design, we could discriminate between similar small organic molecules and observed no significant cross selectivity. Therefore, the MIP array sensor platform with HTM as a readout technique has the potential to become a low cost analysis tool for bioanalytical applications.

# Samenvatting

In deze these worden de eerste stappen beschreven die gemaakt werden bij het maken van een biomimetrische sensor array voor de detectie van kleine organische moleculen via de heat-transfer method (HTM). De heat-tranfer methode berust op veranderingen in de warmte geleiding veroorzaakt door binding van target moleculen op de MIP receptoren. Deze techniek kan voor een tegen een lage kostprijs worden geïmplementeerd aangezien er slechts twee thermocouples en een PID gestuurde warmtebron benodigd zijn. Een nieuw model flow cell wordt ontworpen welke vier afzonderlijke segmenten bevat met elk een volume van 2.5 µL. Deze nieuwe flow cell staat toe om vier metingen tegelijkertijd op eenzelfde substraat te doen alsmede een correctie voor niet specifieke binding binnen hetzelfde staal toe te passen. De quadranten van de sensor worden functioneel gemaakt met MIPs voor serotonine, histamine en L-nicotine, aangehecht op een gespincoate MDMO-PPV laag.

Serotonine en histamine zijn beide essentiële neurotransmitters welke nodig zijn voor een breed spectrum aan fysiologische processen. Naast hun fysiologische functie zijn serotonine en histamine biomarkers voor een aantal ziekten zoals inflammatoire darmziekte (IBS). Hoewel serotonine en histamine vergelijkbare functionele groepen hebben, verschillen ze in afmeting. L-nicotine is gekozen vanwege de afmetingen, welke corresponderen met histamine. De combinatie van deze drie target moleculen kan de specificiteit van de MIPs voor zowel functionele groepen als formaat aantonen.

Na verificatie experimenten worden twee MIP arrays gemaakt die onderscheid konden maken zowel tussen histamine en serotonine als tussen histamine en L-nicotine. Als proof of principle experiment wordt een array gemaakt welke een serotonine MIP en NIP bevat. Deze array in combinatie met een flow cell, waarin een capillaire pomp voor bloed was geïntegreerd, blijkt in staat te zijn om menselijk bloed waaraan serotonine is toegevoegd te kunnen detecteren

Met de verbeterede flow cell voor MIP arrays is het mogelijk om kleine organische moleculen van elkaar te onderscheiden met een MIP array zonder significante kruis selectiviteit. Daarmee heeft het MIP array sensor platform met de heat-transfer method als uitlees methode het potentieel om een goedkope analyse middel te worden voor bioanalytische applicaties.

# Chapter 1: Introduction

Chemical sensors that can be customized to a specific analyte are of interest for areas such as purification and separation (1), biosensors (2,3), drug delivery (4), diagnostics (5) and environmental testing. Currently monoclonal antibodies are used for many of these applications. To make a monoclonal antibody, the antigen of choice is injected into an animal. Often, mice are used as animal of choice. B-cells producing the chosen antigen are taken from the animal, after selecting adequate B-cells these are hybridized with myeloma cells to form a hybridoma. A hybridoma, a hybrid between a cancer cell and normal B-cell, will proliferate and produce the antigen of choice. A simplified graphical representation can be found in Figure 1.1.

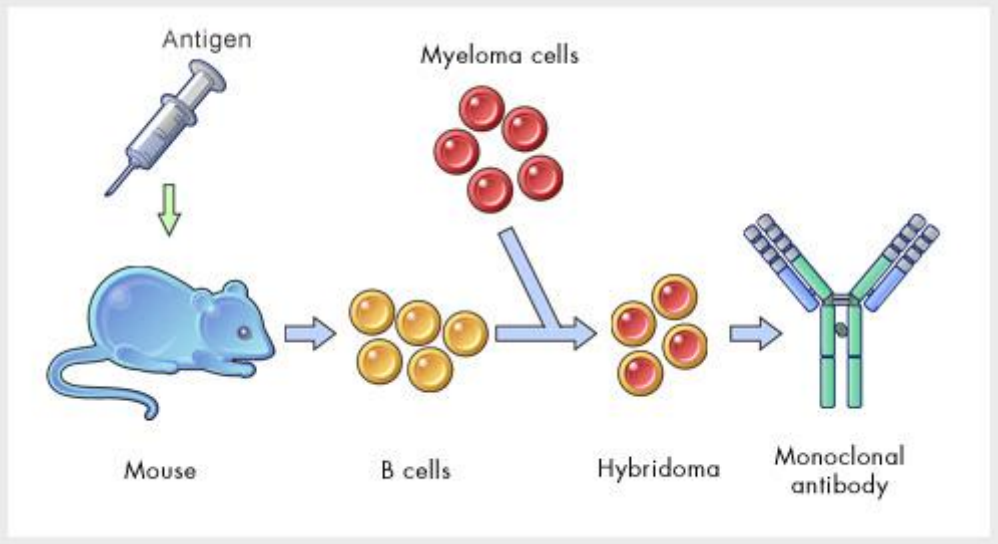


**Figure 1.1,** production of monoclonal antibodies from mouse B-cells.

The traditional approach to produce these necessary sensing elements is laborious and resource intensive. Another problem is that not every antigen can be used due to problems with toxicity or due to fact for some molecules it is impossible to make antibodies because they are endogenous. Besides practical reasons, the use of animals for the production of antibodies is subject of debate for ethical reasons.

Molecularly imprinted polymers (MIPs) offer a solution to these problems as they are relatively straightforward and low-cost to design and produce (6,7). MIPs are synthetic receptors and can be synthesized by copolymerizing functional monomers with crosslinker monomers in presence of the template molecule (8). During production, template and monomers will form a prepolymerization complex by both covalent and non-covalent interactions such as n-n interactions, hydrogen bonds, ionic interactions, hydrophobic effects and van der Waals forces. With the addition of the crosslinker monomers, a polymer shell will form around the template molecule. Removal of the template molecules by polar solvents creates nanocavities with a high affinity and selectivity for the template molecule (9). A graphical representation of this process is shown in Figure 1.2. Non-imprinted polymers (NIPs), which can serve as a reference, are synthesized in a similar fashion but without the presence of the template molecule.

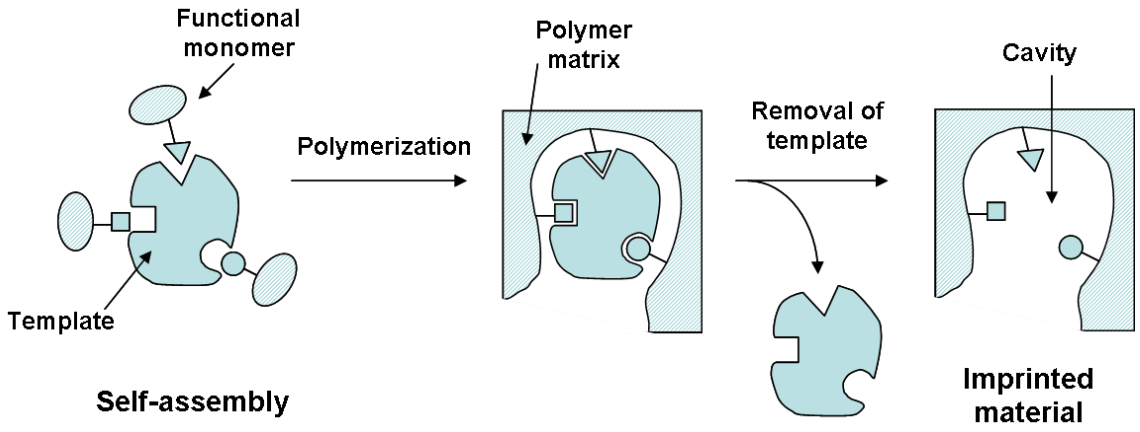


**Figure 1.2,** method of synthesizing molecularly imprinted polymers by copolymerization of template and functional monomers followed by template removal.

The MIP receptors can be prepared for a broad spectrum of molecules ranging from ions (10) and neurotransmitters (11) to larger biomolecules such as proteins (11) or even cells (12). Selection of the optimal functional monomers can be done with computational modeling which allows a fast determination of monomers tailored to a specific analyte (13). Other advantages of MIPs are their resistance to heat and pH (14,15). The ability to re-use MIPs that were synthesized in a non-covalent manner can be an advantage depending on the application (16).

For many years the DNA microarray has been the tool of choice for high throughput gene expression analysis. This method utilizes an array of fixed DNA spots (probes) that are able to bind fluorescently labeled DNA fragments (target) from the sample of choice. After hybridization of target and probe DNA, the array can be scanned. The fluorescent signal of each spot corresponds to the amount of bound target DNA, with this information conclusions about gene expression can be made.

While the DNA microarray has been successfully integrated into biomedical research for high throughput analysis (17), there are only sparse examples to be found in literature for MIP arrays. The first MIP microarray was reported by Shimizu et al. in 2004 (18). They used one non-imprinted polymer and seven molecularly imprinted polymers for biogenic amines and were successful in constructing a colorimetric binding assay. Takeuchi et al. (19) made use of UV-vis spectroscopy to detect a change in analyte concentration. Even though they were able to extend the method from small organic molecules to proteins, high levels of cross-reactivity were observed. Qiu et al. employed a chemiluminescence sensor array for the detection of benzenediol isomers based on graphene-magnetite MIPs. However, this method requires the use of a fluorescent marker which complicates the readout technique due to the need of a confocal microscope and expensive markers. Hawari et al. (20) developed an electrochemical method by utilizing interdigitated electrodes (IDE) as sensor platform. This sensor can be exposed to mango volatiles which causes a shift in capacitance. The response of this sensor can be correlated to the ripeness stage of the mangos in the sample. However, both optical and electrochemical techniques require expensive equipment and the analysis of the measurements is often non-straightforward.

To simplify the analysis of results, this research describes an array format for the heat-transfer method with proof-of-principle experiments performed on the target molecules histamine, serotonin and L-nicotine (Figure 1.3).

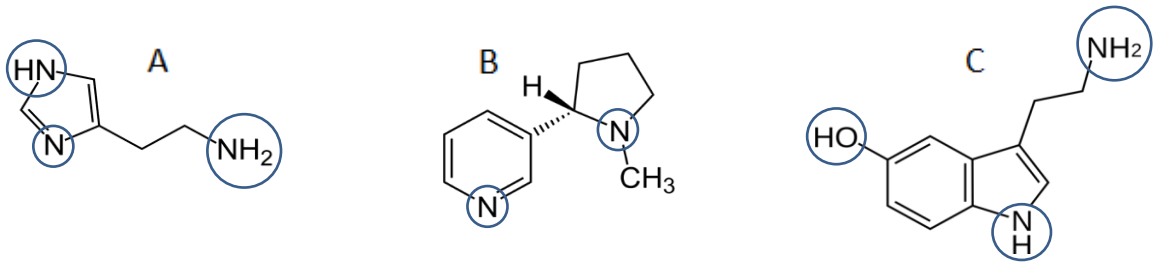


**Figure 1.3,** chemical structure of histamine (A), L-nicotine (B) and serotonin (C). Functional groups are indicated with circles.

The novel heat-transfer method (HTM) has been proposed as a low-cost method to detect small organic molecules with MIP receptors (21,22). The heat-transfer method replaces the often expensive read-out devices with two thermocouples, a proportional-integral-derivative (PID) controller, and an adjustable heat source. In combination with MIPs the heat-transfer method relies on changes in heat transfer through the MIP particles upon binding of target molecules. Prior to the binding event between MIP and target molecules, heat can flow through the open cavities in the MIP particles. However when target molecules bind to the cavities, the heat flux through the MIP decreases. An artist impression of this effect can be seen in Figure 1.4.

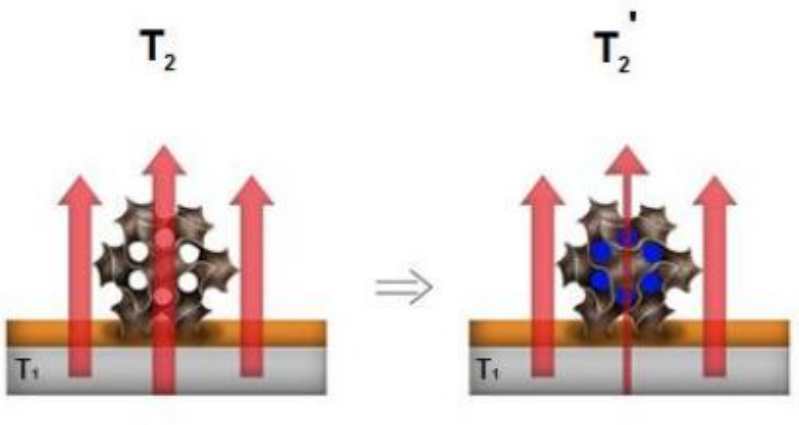


**Figure 1.4,** Pore-blocking model of the MIP receptor.

This effect is explained by the "pore-blocking model". If only the temperature difference between $T_1$ and $T_2$ is used for measurements, variations in power necessary for keeping the heating block at a stable temperature would affect the measurement. Since the voltage required to keep the temperature of the heater is logged by the PID controller and the resistance is a known constant, it becomes possible to calculate the power that was required to keep $T_1$ stable. By using the power it is possible to remove environmental effects such as variations in room temperature. The copper block, as seen in Figure 1.5, is kept at a constant temperature. After calculating the power necessary to keep the heating block at a constant temperature, this value can then be used to obtain the thermal resistance ($R_{th}$) for each sensor. $R_{th}$ is defined as:

$$R_{th} = (T_1 - T_i)/P$$

In which P is the power in Watt (W), $T_0$ is the temperature in degrees Celsius (°C) of the heat sink (copper block), and $T_i$ with i=1,2,3,4, is the temperature of the fluid in each sensor in degrees Celsius (°C).

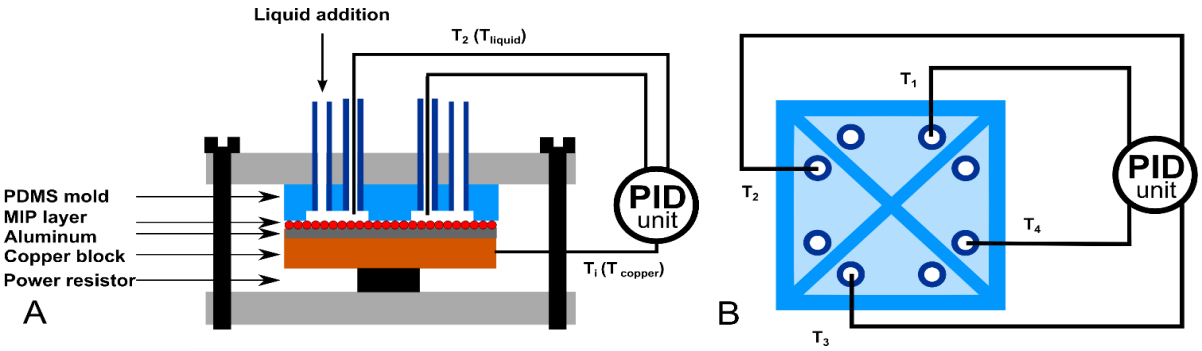


**Figure 1.5,** schematic representation of the new flow cell. The black lines indicate the thermocouples used for the $R_{th}$ measurements. Figure 1.5A shows a side view of the whole setup, only two of the four quadrants are shown for clarity. Figure 1.5B shows a top view of the PDMS stamp used to create four separate sensors.

Although the previous sensor platform allowed detection of physiologically relevant concentrations of various small molecules, it was necessary to use large amounts of sample volumes (110 µl) and only a single sample could be measured (11,12). In this research, an optimized flow cell design capable of measuring up to four samples simultaneously is presented. This allows for functionalization with MIPs for different targets onto a single sensor substrate along with a decreased measurement time. The required sample volume is also reduced to 1 µl, diminishing the need for large amounts of analyte which is beneficial for biological samples which are often hard to acquire in large quantities.

The chosen neurotransmitters histamine and serotonin are required for the function of various physiological processes (23). Serotonin and histamine also play a role in diseases such as irritable bowel syndrome (IBS), a disease that affects 10-20% of the population in western societies (24). Symptoms are discomfort in the form of chronic abdominal pain, discomfort, diarrhea or constipation, bloating, and alteration of bowel habits. Patients also have a higher percentage of missed days of work than healthy subjects (11,3% vs 4,2%) due to their illness (25). The number of doctor visits related to IBS in the United States lies between 2.5 and 3.4 million per year (26). Together, these doctor visits result in 2.2 million prescriptions being written out for the patients (27) along with higher overall health costs (28). Overall for the United States, this leads to €1.6 billion of direct costs due to IBS and €19.2 billion in indirect costs for society (29). Patients themselves show a health related quality of life comparable to diabetes patients which shows that IBS results in a serious impairment of the patient's quality of life (30).

One of the causes of IBS is thought to originate from a disturbed serotonin and histamine concentration in the bowels of the patient. Research has shown higher numbers of enterochromaffin cells and differences in mucosal serotonin metabolism in IBS patients compared to healthy subjects (31). In the gut, serotonin is stored in the enterochromaffin cells where it can be released after mechanical or chemical stimulation (23). Upon contact between mucosal nerve endings of the enteric nervous system and serotonin, the motor and secretory functions of the intestines will be affected (32). Histamine is found in the mast cells present in both intestinal mucosa and circulation. These cells can be activated by the stress hormone corticotrophin. Upon activation, the mast cells release among others histamine which can be found in concentrations twice as high as in healthy subjects (33). The level of histamine and serotonin in blood and/or intestinal fluid is currently used as one of the indicators of IBS. At present, laboratories use HPLC, gas chromatography and ELISA tests for the detection of serotonin and histamine (34–36). While these techniques offer a low detection

limit and a high specificity, the first two are expensive and the ELISA technique is labor intensive. The MIP-based serotonin and histamine sensors offer detection limits as low as 10nM in liquid samples (11) which includes the relevant levels of both substances related to IBS while being significantly cheaper and faster than the current laboratory standards. The chemical structure of histamine and serotonin is similar due to the presence of an imidazole ring and an amine functionality. However, their size is different which is why L-nicotine was chosen as a third template molecule. L-nicotine is the main addictive substance in tobacco (37) and has approximately the same physical dimension as histamine. The combination of these templates takes both chemical similarity and size into account. The small organic molecules will only cause a response in the MIP receptors targeted towards them while causing no response in the other MIP receptors. For these experiments, a concentration of 1 mM target molecule in PBS (pH = 7.4) was chosen to evoke a clear response. To determine the detection limit of the MIP sensors concentrations down to 100 nM were used. The low cross selectivity, along with the miniaturization of the setup and reduction of measurement times, are important steps for the implementation of the MIP sensor array for diagnostic applications.

A proof of concept application would be the detection of serotonin in whole blood. A MIP array containing at least one MIP for serotonin and a NIP to correct for non-specific binding would be a minimum requirement to give a reliable result. However, the array formatted flow cell requires knowledge of the setup and medical training to handle human blood. Therefore, a setup into which a drop of blood is deposited without any syringes or pumps would be ideal. Such an application is built and tested in this research.

# Chapter 1 : Introduction

# Chapter 2: Materials & Methods

## *2.1: Cleaning of the sensor substrate*

The sensor substrate consists of aluminum sheet metal with a thickness of 1 mm cut to a size of 1 x 1 cm. To remove scratches and tooling marks, they were polished by means of wet sanding with grit sizes up to P4000 to achieve a mirror finish. To get rid of any grease or contaminants, the substrates were put into an ultrasonic bath with acetone for 5 minutes. After rinsing the substrates with isopropanol, the samples were dried with nitrogen.

## *2.2: Spincoating*

To apply an adhesive layer to the substrates, a layer of $OC_1C_{10}$-PolyPhenyleneVinylene (MDMO-PPV) was spin coated onto the substrates. MDMO-PPV, synthesized according to reference (38), was dissolved in chlorobenzene to achieve a 0.7% (weight percentage) solution. The spin coating was performed under a nitrogen atmosphere at 3000 rpm, 500 $m/s^2$ for 30 seconds. The layer thickness of the MDMO-PPV was determined to be approximately 100-200 nm.

## *2.3: MIP and NIP synthesis*

The synthesis of the MIP particles was performed according to the following recipe. A mixture of the functional monomers, crosslinker monomers and initiator was dissolved in the porogen together with the template molecule. After degassing the solution, polymerization was initiated either by UV-light or by heat. After polymerization, the compound was ground to obtain a powder and the template was removed by Soxhlet extraction. The non-imprinted polymer (NIP) was prepared according to the same recipe except for the addition of the target molecule. Therefore, the NIP can be used as a negative control. For full details on the synthesis procedure, see references (11,39,40).

## *2.4: Application of MIP and NIP particles.*

A polydimethylsiloxane (PDMS) stamp was used to transfer a thin layer of MIP or NIP powder to the substrate. To do this, the PDMS stamp was pressed into the corresponding MIP or NIP-powder and subsequently onto the adhesive layer in order to transfer the particles onto the substrate. By using different stamps and stamp sizes it is possible to either cover the entire surface of the substrate with particles targeted to a certain template, or to create up to four areas coated with MIPs targeted to different templates. Separation of the segments can be improved by covering parts that should not be stamped with glass slides or by using smaller triangle shaped stamps. The substrates were placed on a hot plate to heat them above the glass transition temperature of MDMO-PPV which allows the particles to partially sink into the softened layer. After letting the samples to cool down, they were rinsed with isopropanol in order to remove particles that are not fixed to the substrate. Particle loading and verification of separation between quadrants was performed with an Axiovert40 inverted optical microscope (Carl Zeiss, Germany).

## *2.5: Design of the sensor setup*

The functionalized substrates were placed on a copper heating block which utilizes a power resistor (22 Ω, MPH20S, Farnell, Belgium) as a heat source. A PID controller regulates the temperature of this copper block. The PDMS flow cell, containing four quadrants with a surface area of 5 $mm^2$ and an inner height of 0.5 mm, is placed on top of the sample. Two Perspex plates clamp the whole setup together with screws that can be tightened to apply a small amount of pressure, ensuring a watertight seal between substrate and PDMS. A miniature thermocouple (type K, diameter 500 µm, TC Direct, The Netherlands) was inserted into the copper block. The temperature ($T_0$) of the copper block is controlled at 37.00 ± 0.02 °C to mimic the human body temperature with a PID (parameters: P= 1, I= 8, D= 0.1) controller that was designed in-house. A thermocouple is inserted into each of the quadrants to monitor the temperature ($T_{1,2,3,4}$) in the liquid at equal height above the sample. To insert the thermocouples to equal depths, adjustments are made to the depth until all liquid temperatures read approximately 33 °C. The liquid temperature, as monitored by the four thermocouples in the liquid and single one in the copper block, is logged by the software once per second. Figure 2.1 shows the schematic design of the sensor setup.

Before the start of every measurement, the flow cell was filled and flushed with phosphate buffered saline (PBS) solution (pH = 7.4) until all air was removed from the flow cell. To gain a stable baseline level, the setup was heated to 37.00 ± 0.02 °C and left to stabilize for at least one hour. After stabilization, 1 ml of PBS containing the template molecules (histamine, serotonin and L-nicotine) at the required concentration was added to each cavity to ensure that the previous liquid is flushed out.

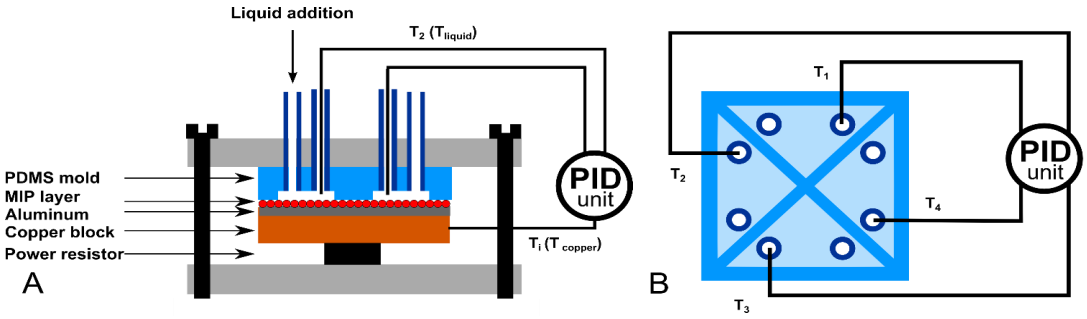


**Figure 2.1,** Schematic side A and top view B of the PDMS flow cell and the four thermocouples. The temperature of the copper, $T_1$ is strictly controlled. The temperature of the liquid ($T_{2,3,4,5}$) in each quadrant is solely monitored.

## *2.6: Heat-transfer method*

The heat-transfer method is based on alterations in thermal resistance ($R_{th}$) due to changes at the surface. Examples of these changes can be denaturation of DNA or binding of target molecules to a MIP layer. A big advantage of the heat-transfer method over classical methods such as HPLC is the low cost at which the HTM can be implemented. With merely two thermocouples, a PID controller/temperature monitor and a power resistor, it is possible to perform $R_{th}$ measurements. The copper block, as seen in Figure 2, is kept at a constant temperature and after calculating the power necessary to keep the setup at a constant temperature, this value can then be used to obtain the thermal resistance ($R_{th}$) for each quadrant.

## *2.7: Capillary flow cell*

In order to make a single shot flow cell, capable of measuring the serotonin concentration in whole blood, a new flow cell was designed. This new flow cell incorporates a passive pumping system based on a capillary pump to remove the need for a pumping system of syringes to add the sample. PDMS was chosen as material to make the flow cell. The advantages of using PDMS are the ease of processing and low price as well as the possibility to make PDMS hydrophilic. A Teflon mold was designed and manufactured with a computer numerical controlled (CNC) mill. The capillaries were made by placing metal pins with a thickness of 1 mm into predrilled holes in the Teflon mold. To create clear edges, glass microscope slides were cut to size and attached to the sides of the mold with scotch tape. After mixing PDMS and placing it in a vacuum chamber to remove air bubbles the mold was filled with PDMS. By placing the mold with PDMS once again in the vacuum chamber, air that might be present between mold and PDMS was removed. After curing the PDMS in an oven at 120 °C, the mold was removed. A biopsy needle was used to cut two holes for thermocouples above the sensor surface, in these holes a thermocouple was inserted and fixed with a few drops of PDMS. After curing at 80 (°C) to attach the thermocouples to the PDMS block, the flow cell was ready. A 3d drawing of the PDMS flow cell can be seen in Figure 2.2.

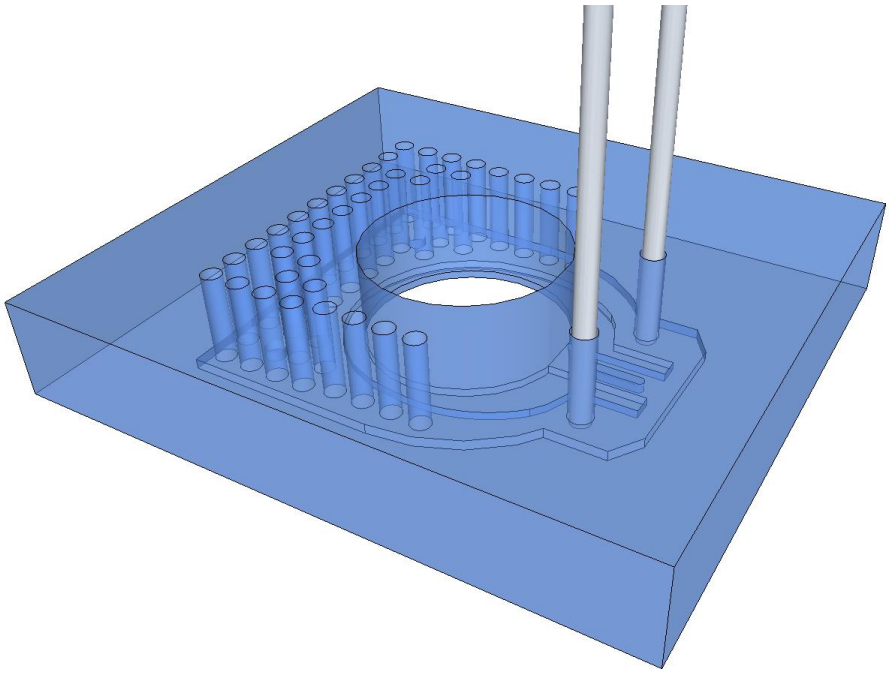

**Figure 2.2,** PDMS flow cell with thermocouples (grey tubes). A large liquid reservoir can be seen in the middle of the PDMS flow cell with a split channel leading to the sensor surfaces below the thermocouples. Further down the channel an area with a capillary pump can be seen. For whole blood the height of the channels should be between 0.6 mm and 1.0 mm.

A 3 cm by 3 cm aluminum block with a thickness of 3 mm was used as heating element. This heating block uses a 22 Ω power resistor (MPH20S, Farnell, Belgium) as a heat source. The back of the heating block is encapsulated in PDMS to create a flat surface and reduce heat loss at the backside.

Due to the larger size of the capillary flow cell, new 3 cm by 3 cm aluminum plates were cut from 1 mm thick sheet metal. Cleaning, spin coating and application of MIP and NIP was performed as

described in chapter 2.1-2.4. Half the substrate was covered with MIPs for serotonin and the other half with a NIP of the same material as the serotonin MIPs.

Upon stacking of the heating block, sensor substrate and flow cell together, each of the two thermocouples is positioned either above the MIP or the NIP particles. The setup is allowed to stabilize for at least one hour without liquid inside before a single shot of whole blood sample is added to the setup.

### *2.8: whole blood preparation*

In order to acquire blood without the need for medical training, as was required by the design criteria, blood was taken from a finger by means of an Onetouch Ultrasoft pen needle. This pen needle is commonly used by diabetes patients to acquire a few blood droplets, as required for insulin testing. To avoid blood clotting, 5 µl of heparin was added to an Eppendorf tube prior to adding the blood. In order to remove offsets in serotonin concentration between experiments and to ensure a response, 50 µl of 1 mM serotonin in PBS (pH = 7.4) was added to the heparin, the blood was added to this solution. The end concentration of serotonin in the blood sample is approximately 250 µM. Small variations are possible due to variation in serotonin levels of the test subjects blood and the amount of blood gained.

# Chapter 3: Results

## *3.1: cross contamination analysis*

To verify the possibility of functionalizing four independent segments without bringing particles outside of the stamped areas, an array was prepared onto glass and analyzed with a microscope.

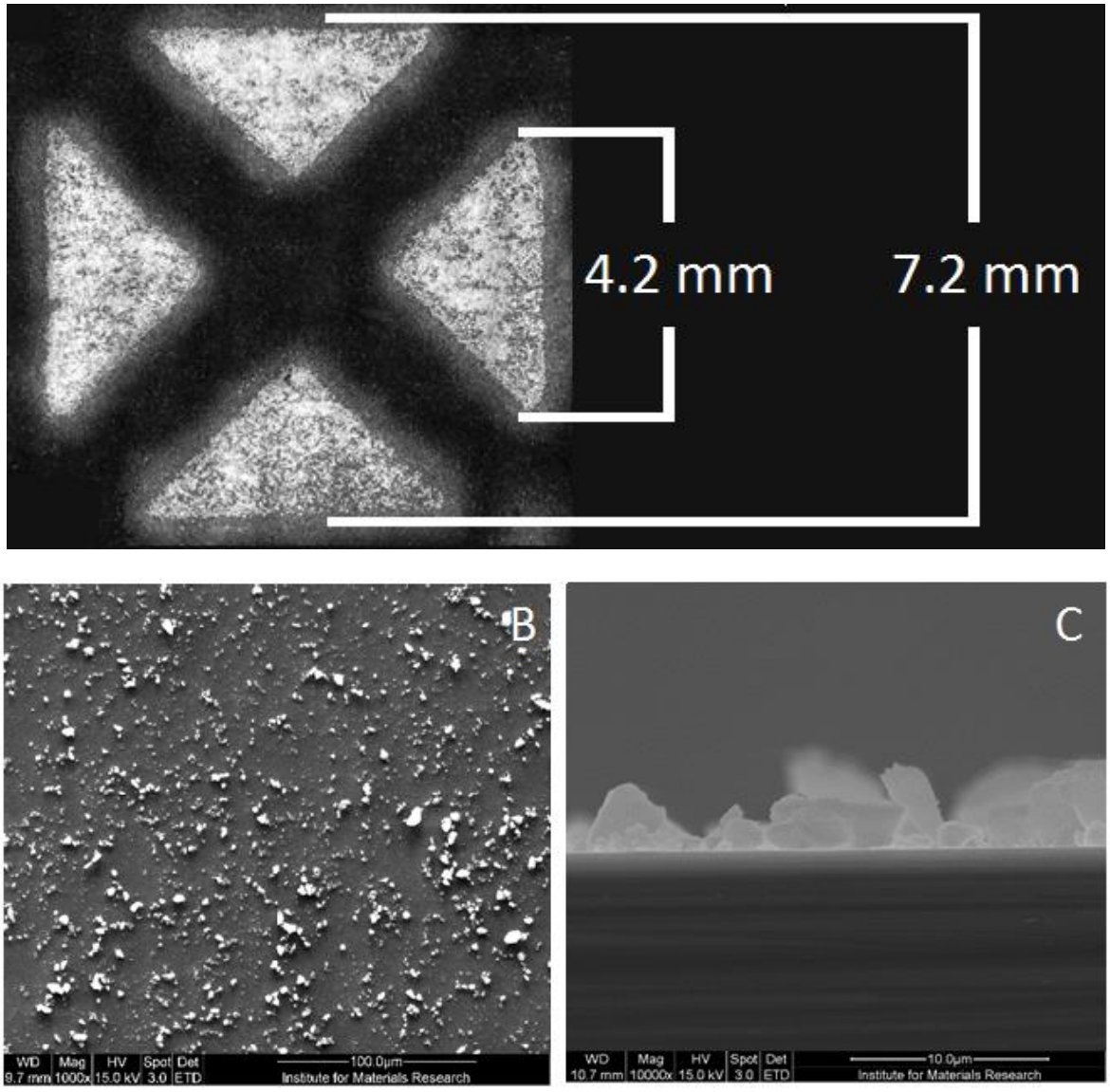


**Figure 3.1,** *The MIPs are adhered to the surface into four segments with a length of 4.2 mm. The interspacing between segments was 2 mm and the total size corresponds to 7.2 mm. The bright spots correspond to areas where the MIP particles stick to the glass slide. The optical image was obtained with an Axiovert microscope of Carl Zeiss. B shows a Scanning Electron Microscopy (SEM) image which was zoomed into a quadrant containing one type of particles. C shows a side view of the sample.*

The images shown in Figure 3.1 demonstrate the result of stamping onto a glass slide and indicate that the four triangles are well defined. Since there appears to be no application of particles on surfaces outside of the stamped triangles, an analogous procedure was performed onto an aluminum substrate. The images taken are shown in Figure 3.1. By optical microcopy in combination with Image J

software the surface coverage was determined to be around 28% ± 1% while the particles are approximately 5 µM big.

### *3.2: Dose response of the MIP sensor for nicotine*

A substrate was functionalized with solely L-nicotine MIP particles in order to determine the limit of detection (LOD). After stabilization in PBS (pH = 7.4) for one hour, five solutions containing increasing amounts of L-nicotine in PBS were added. The five L-nicotine in PBS solutions had concentrations of 100 nM, 1 µM, 10 µM, 100 µM and 1 mM.

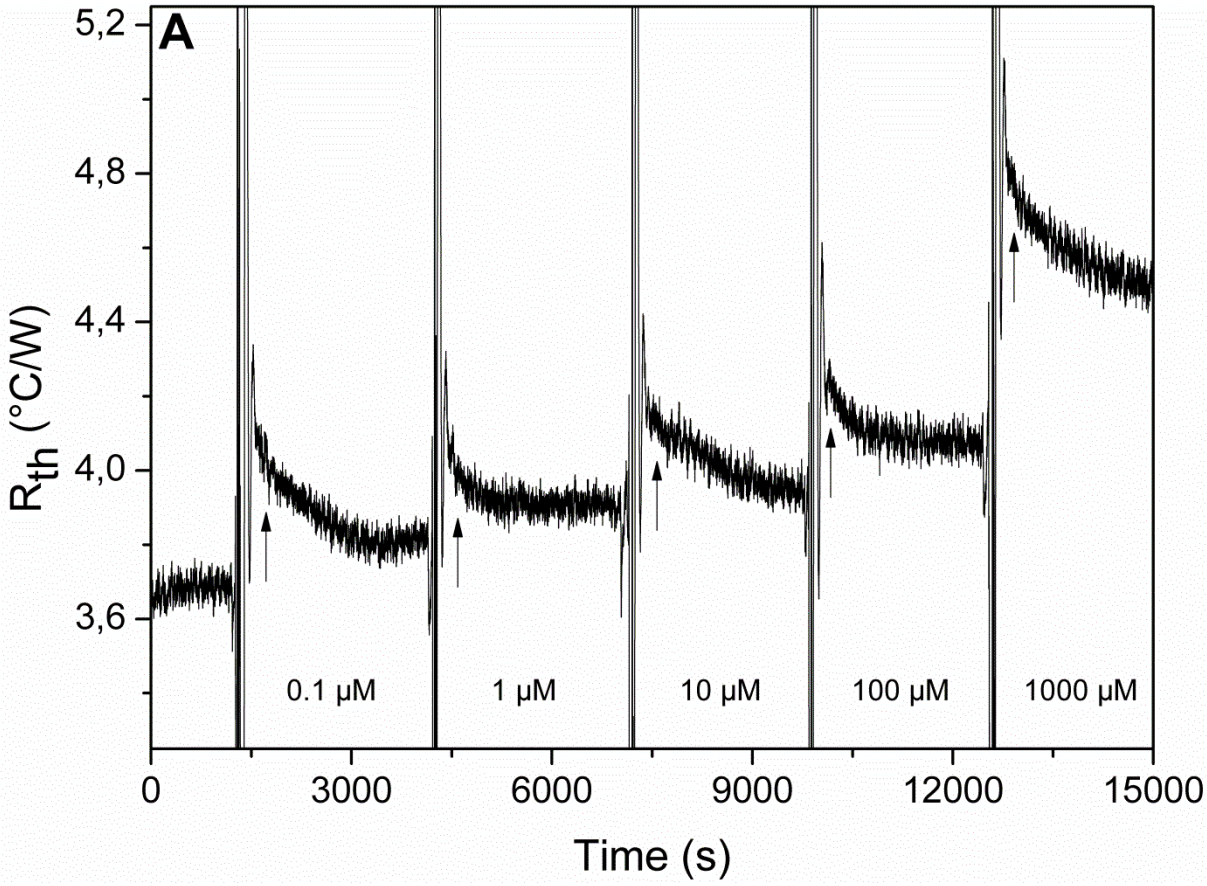

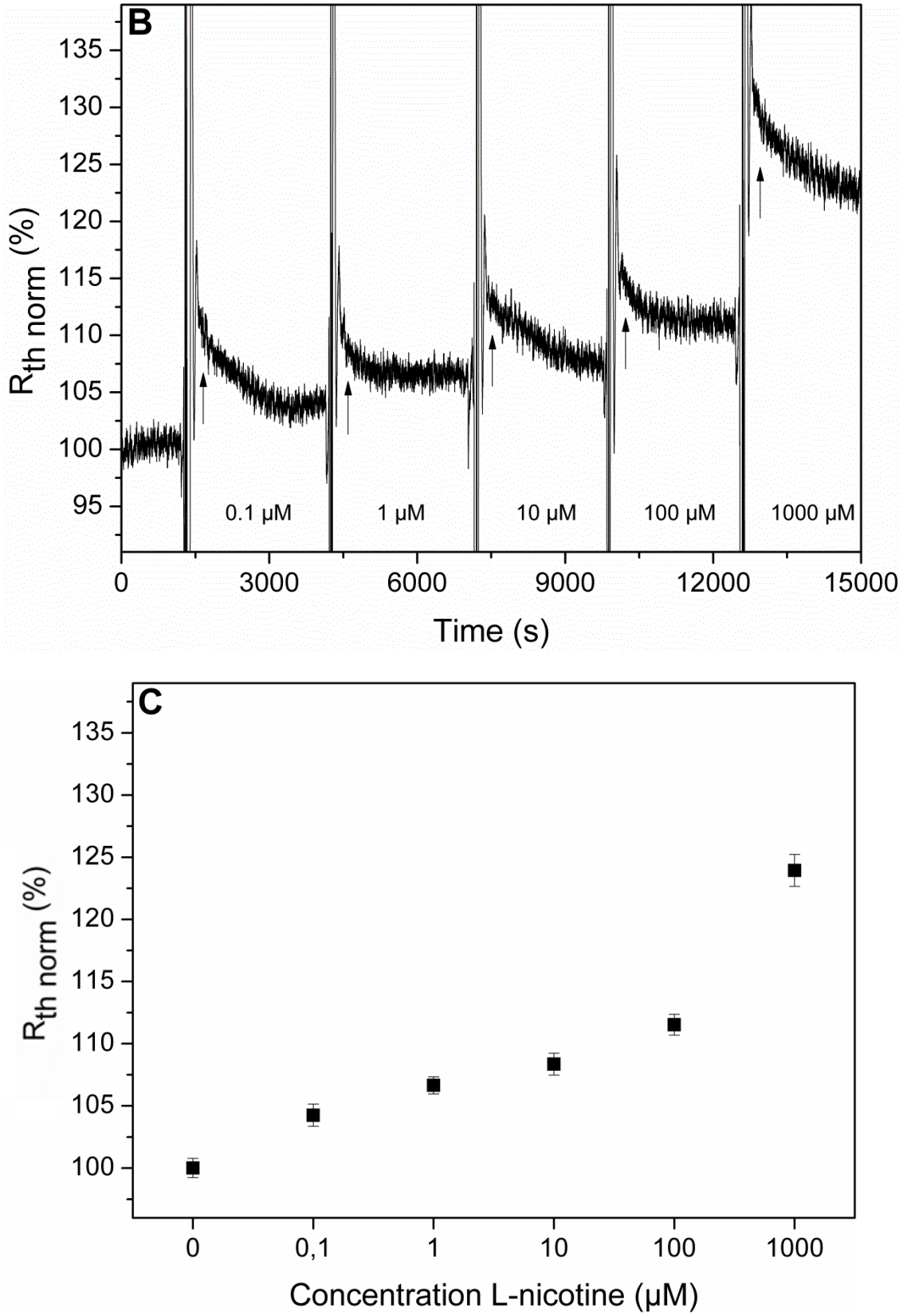


**Figure 3.2** A shows the raw $R_{th}$ data for five solutions with an increasing L-nicotine concentration. B displays the normalized data of A expressed as a percentage of the initial $R_{th}$ in PBS. C is the dose-response curve in which the concentration versus the relative response in $R_{th}$ is plotted.

The data shown is taken from one of the quadrants for clarity. Figure 3.2 A displays the raw $R_{th}$ and the effects of the sequential additions of the increasing L-nicotine concentrations. In Figure 3.2 B the normalized $R_{th}$ is shown. The normalized signal removes the offset between channels due to slight variations in the distance between thermocouple and substrate. The normalization was performed by dividing each $R_{th}$ value (time = n) by the initial baseline (time = 0) in pure PBS and multiplying the outcome by 100 to get a normalized starting value of 100 %. The formula for this calculation reads:

$$R_{th\,norm}(\%) = \frac{R_{th\,(t=n)}}{R_{th\,(t=0)}}\ x\ 100$$

From the normalized data the average of every period was calculated as well as the standard deviation. The average $R_{th}$ values and standard deviations are plotted in Figure 3.2 C

The first addition of L-nicotine in PBS (100 nm) caused an increase in Rth of 4.2 % (± 0.9 %). The maximum increase was seen at a concentration of 1 mM, with an increase of 24.0 % (± 1.3 %) relative to the initial baseline level. Via this dose-response curve, the limit of detection (LOD) for the MIP sensor can be estimated. The LOD is defined as the concentration where the response equals three times the noise on the base line level. To determine this, a fit using the formula:

$$R_{th} = X + Y * log(\frac{C}{1\ \mu M})$$

was performed for the concentration regime 0.1–100 µm resulting in a $R^2$ of 0.98. The parameters used for this fit were X = 92.40 and Y = 1.02. This results in a LOD of 30 nm, comparable to a fully optimized setup which has been used in previous measurements (41).

### *3.3: L-nicotine MIP array*

To assess the consistency of the data over the quadrants, an experiment with MIPs for L-nicotine was performed. Three segments, imprinted for nicotine have been created, together with one reference channel. All channels were left to stabilize in PBS buffer (pH = 7.4) for an hour. After the stabilization period, 1 ml solution of 1 µM L-nicotine in PBS was added to the four quadrants.

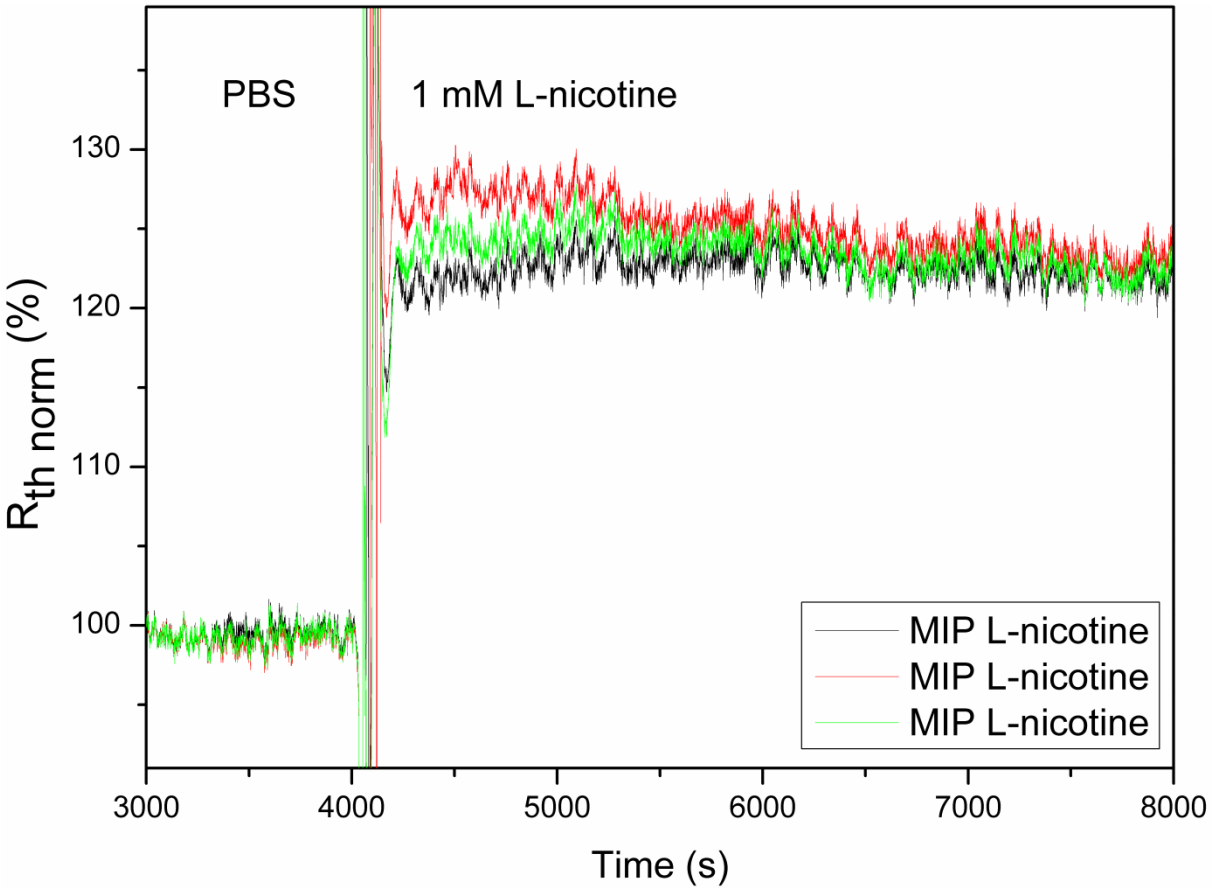


**Figure 3.3,** normalized $R_{th}$ of three identical L-nicotine MIPs before and after being exposed to 1 mM L-nicotine.

In Figure 3.3 the data from the three MIP-stamped channels is shown. The three channels all show an increased $R_{th}$ after the addition of the target molecule close to that of the other channels. This indicates that the quadrants give a similar response when exposed to equal conditions.

### *3.4: Array format for three MIPs and one NIP*

After assessing three identical MIPs, a substrate with one NIP and three different MIPs was made. The three MIPs were targeted towards L-nicotine, serotonin and histamine while the NIP was of the same material as the L-nicotine and histamine MIPs. After allowing the sensor to stabilize in PBS (pH = 7.4) for 60 minutes, each channel was flushed with an addition of the same target molecule the MIP in that channel was designed for. Due to the design of the flow cell each channel is separated from the others, there can be no mixing of liquids inside the setup. Every addition consisted of 1 mL PBS with the target molecule at a concentration of 1 mM. After the addition, a clear increase in the $R_{th}$ value can be observed for all three channels as seen in Figure 3.4. It can also be observed that all three channels have an almost equal increase even though the MIPs are targeted to different target molecules in each channel. The NIP channel remains at baseline as was expected.

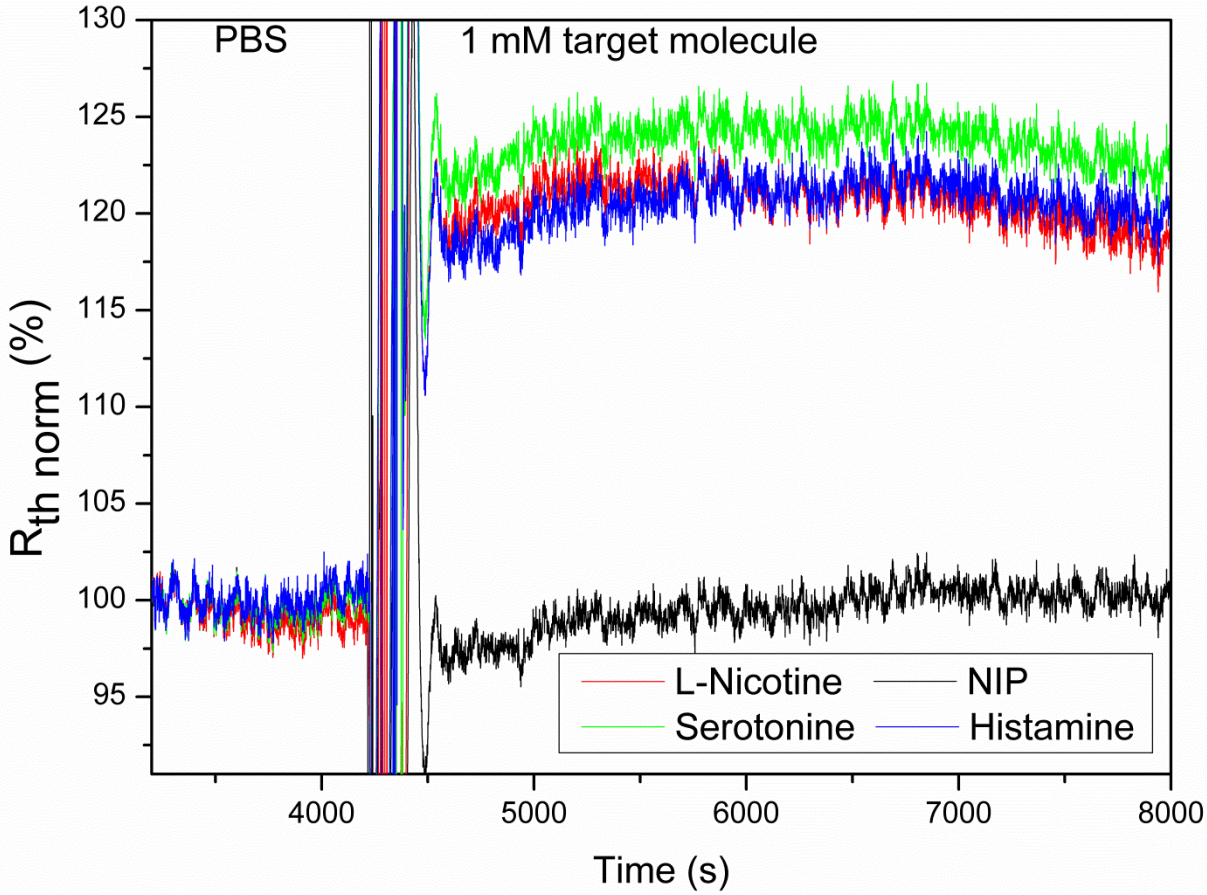


**Figure 3.4,** normalized $R_{th}$ of three MIPs and one NIP before and after exposure to their target molecule.

### *3.5: Sequential addition of target and non-target molecules*

To test the effect of solutions with target or non-target molecules, a substrate was made where 50% of the quadrants were prepared with L-nicotine, histamine or serotonin MIPs and the other half with a different MIP. After a stabilization period of one hour an addition of 1 mL PBS (pH = 7.4) containing 1 mM of either target or non-target molecule was added to both channels. The first experiment was performed with histamine and L-nicotine MIPs.

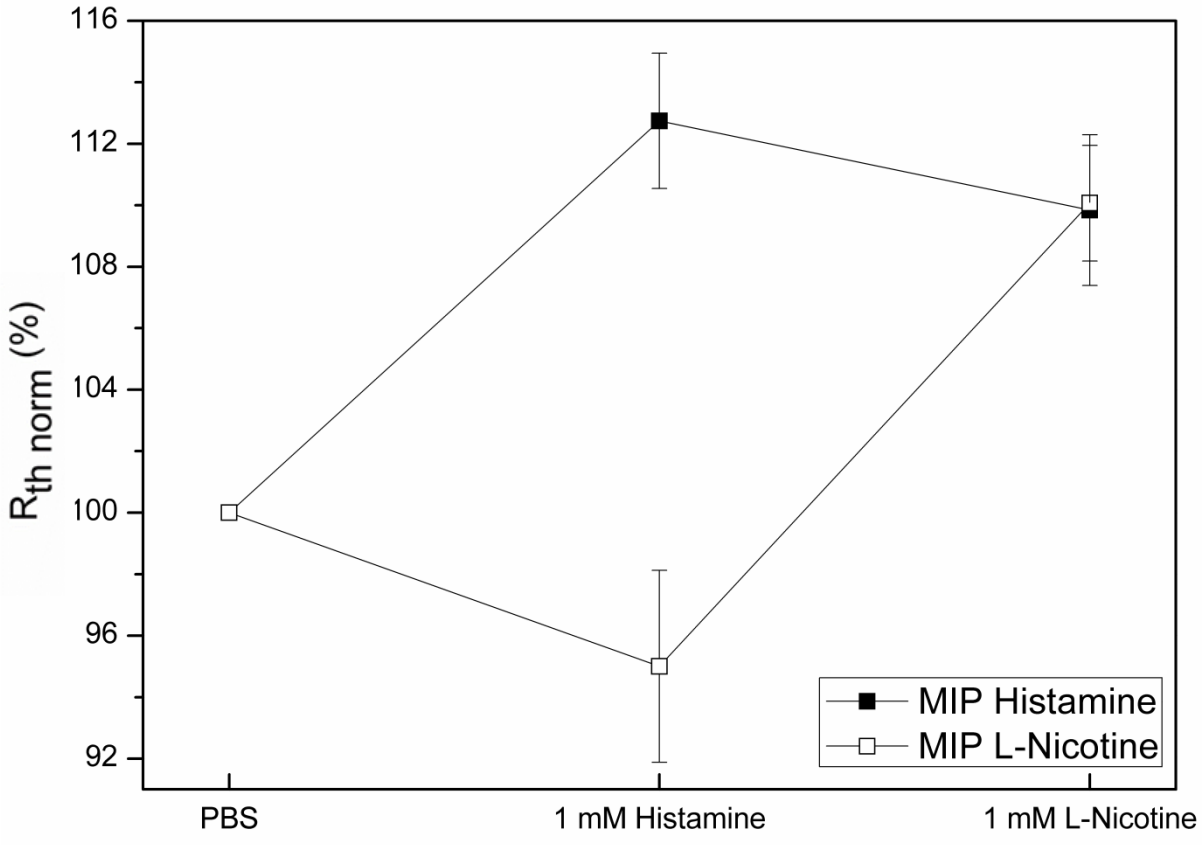


**Figure 3.5,** Thermal response curve of histamine and L-nicotine sensitive sensor spots upon exposure to a solution with a concentration of 1 mM histamine (first) and 1 mM L-nicotine (second) in PBS buffer.

After stabilization in PBS (pH = 7.4) for one hour, a solution of 1 mM histamine in PBS was added to the setup. This addition causes the histamine MIP channel to rise in $R_{th}$ while the L-nicotine MIP channel does not show a significant change in $R_{th}$. The second addition consisted of 1mM L-nicotine in PBS which resulted in an increase in $R_{th}$ for the L-nicotine MIP channel while the histamine MIP channel did not change significantly. The averages shown in figure Figure 3.5 were calculated over the periods where the temperature had stabilized; from shortly after additions until shortly before the next addition. All error bars were calculated over the same period as taken for the average value. The second experiment was performed with serotonin and histamine MIPs. The setup was filled with PBS and allowed to stabilize for one hour. After stabilization, 1mL of 1 mM serotonin was added to the setup resulting in an increase in $R_{th}$ of the serotonin MIP while the histamine MIP remains at a lower $R_{th}$. A second addition was done with 1 mM histamine which resulted in an increased $R_{th}$ for the histamine MIP while the serotonin MIP remained at the same level as can be seen in Figure 3.6.

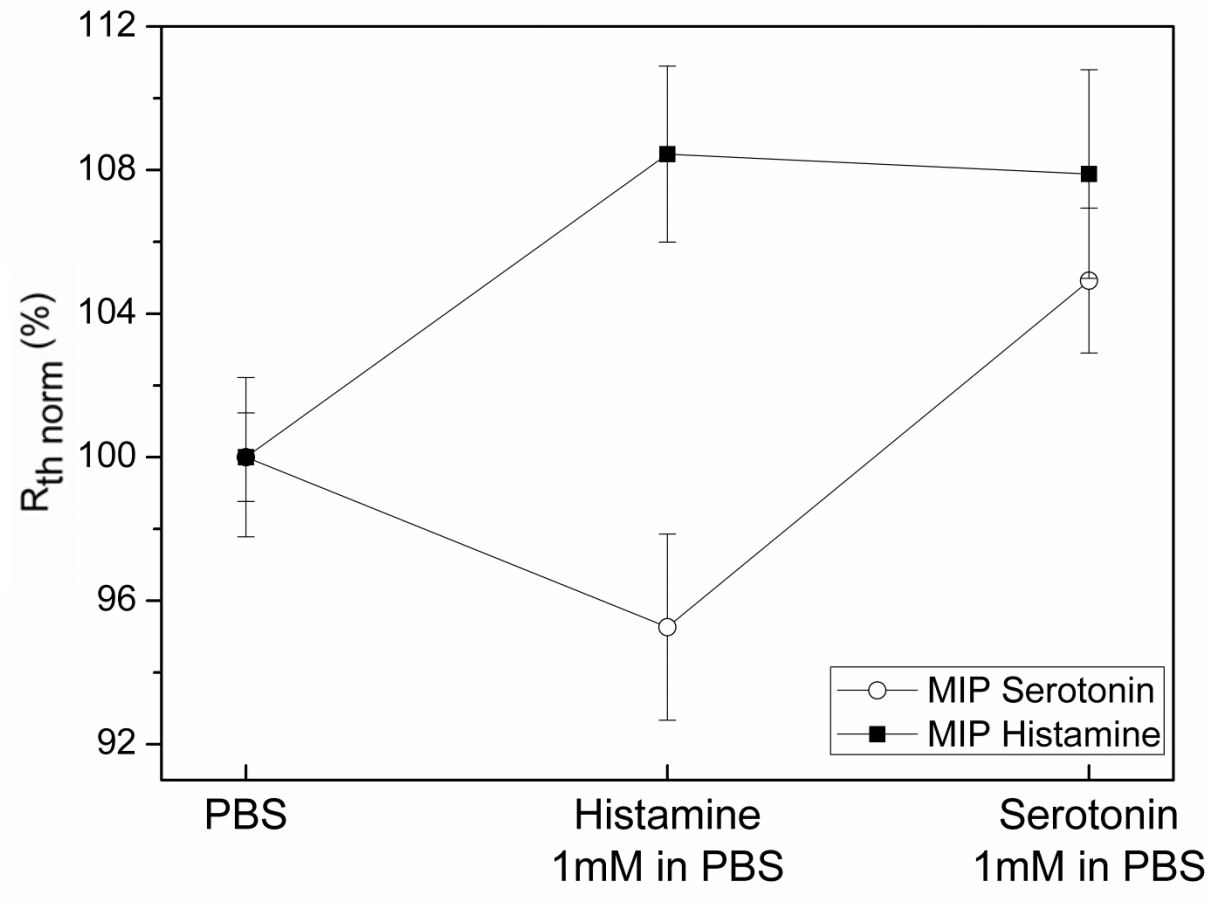


**Figure 3.6,** thermal response of histamine- and serotonin-sensitive sensors spots upon exposure to a solution with a concentration of 1 mM histamine (first) and 1 mM serotonin (second) in PBS. The experiment has been performed by sequential additions of the target molecules to the sensor quadrants without intermittent washing steps.

### *3.6: Correction for non-specific binding*

To correct against non-specific binding, non-imprinted polymers (NIP) can be used. Having a NIP on the same substrate as the MIP reduces the variation between samples. To verify the effectiveness of adding a NIP to the array, a substrate was prepared where half of the segments were functionalized with a MIP for histamine and the other half with a histamine NIP. After a stabilization period of one hour with PBS (pH = 7.4), a solution containing 10 µM histamine in PBS was added. The addition of histamine causes an increase in $R_{th}$ for both the MIP and NIP channel. Correction of non-specific binding can be performed by subtracting the normalized $R_{th}$ of the NIP from the normalized $R_{th}$ of the MIP. Earlier research indicated that this correction allows to make the step from a well-controlled buffer solution to biological samples such as saliva, blood and urine (11,12,21). Another advantage is removal of external factors such as fluctuations in temperature of the environment. In Figure 3.7 A the signal after correction for non-specific binding can be seen. Figure 3.7 B shows the average $R_{th}$ value before the addition of histamine and after. It can be seen that the MIP shows a bigger increase in $R_{th}$ than the NIP for the highest concentration.

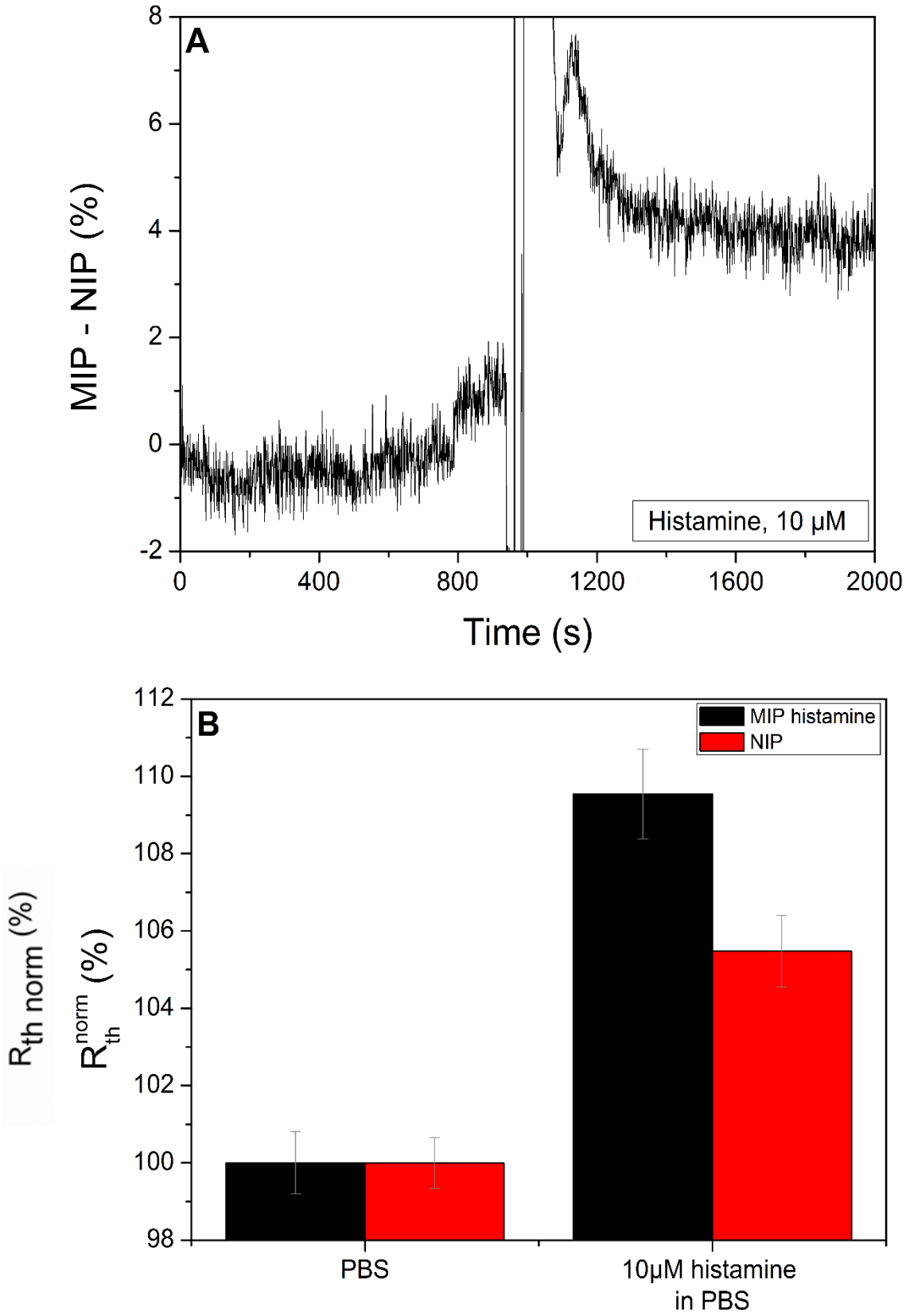


**Figure 3.7,** A, sample onto which both a MIP and a NIP for histamine were applied, was allowed to stabilize with PBS (pH = 7.4). After stabilization the sample was exposed to a solution of histamine in PBS (pH =7.4) with a concentration of 10 µM. Graph B shows the average $R_{th}$ as seen in figure 6A plotted in function of the concentration.

### *3.7: Whole blood measurements*

As correction for non-specific binding is possible, a substrate for the capillary whole blood flow cell was prepared with a MIP and NIP for serotonin. After allowing the setup to stabilize for an hour, the blood spiked with 250 µM serotonin was added to the sensor.

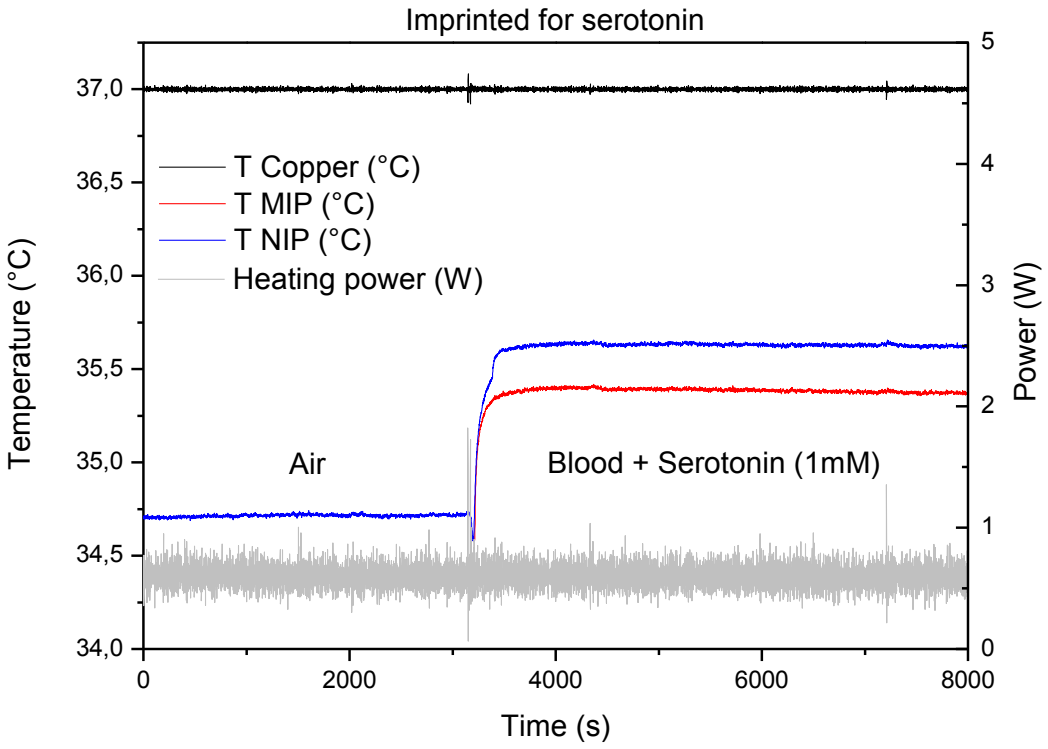


**Figure 3.8,** Effect of whole blood on the temperature as measured by the thermocouples.

The blood caused a decrease in thermal resistance due to the increased thermal conductivity compared to air. The effect of the added liquid on the temperature can be seen in Figure 3.8. Already a deviation between the temperature of the MIP and NIP can be observed due to the MIP layer, which adds another thermal resistance that is higher than that of the NIP layer. To ensure that this effect was not caused by a difference in the distance between thermocouple and substrate, the experiment was repeated with a blank substrate where no difference was seen between channels. Another experiment was conducted where the locations of MIP and NIP were switched, the experiment proved to be successful and the effect can be attributed to the MIP and NIP layer.

By subtracting the NIP signal from the MIP signal, the graph as seen in Figure 3.9 was acquired. An increase in the differential $R_{th}$ can be observed upon contact with whole blood. This indicates that there is serotonin present in the blood.

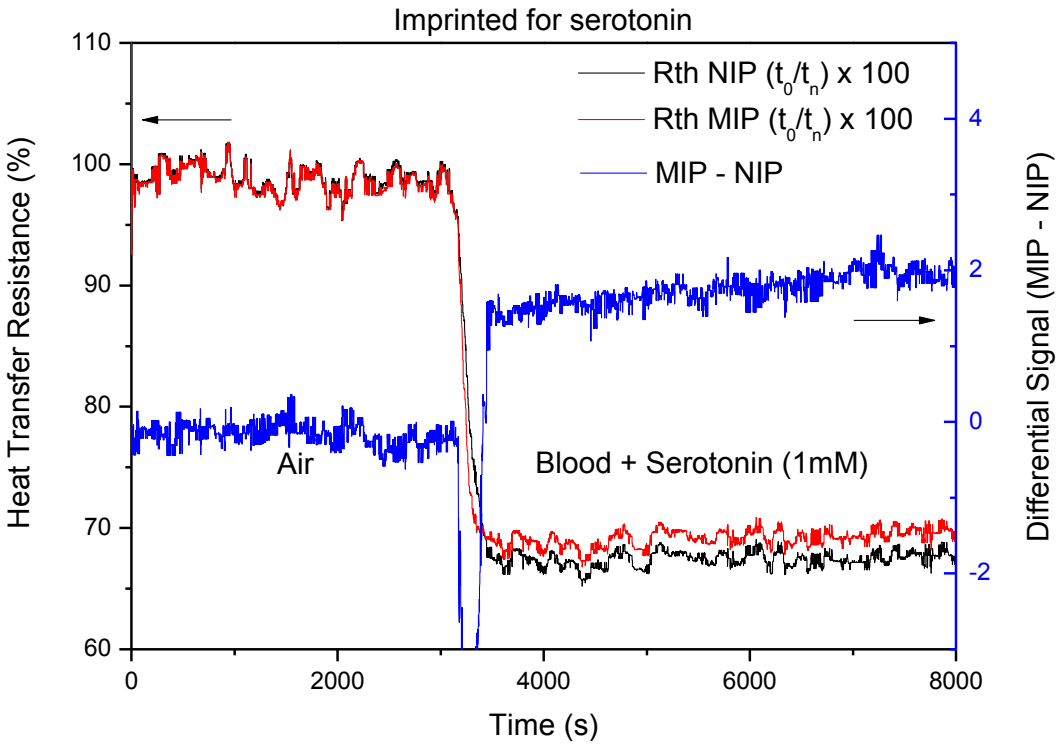


**Figure 3.9,** $R_{th}$ of the MIP and NIP channel combined with the differential signal.

### *3.8: MDMO-PPV versus PVC*

To test the feasibility of PVC as an adhesive layer for attaching the MIPs to the substrates, a substrate was prepared according to the standard procedure. The only deviation from the standard procedure was the use of 0.7% (weight percentage) PVC in tetrahydrofuran instead of the MDMO-PPV. PVC has the advantage of being cheaper than MDMO-PPV as well as not requiring chlorobenzene as solvent. Another sample was prepared with MDMO-PPV to serve as a reference. Due to small variations in the insertion depth of the thermocouples, channels with similar temperatures were matched. This ensures equal conditions except for the difference in adhesive layer. Their average $R_{th}$ over the stabilization period was calculated as well as the standard deviation. Figure 3.10 shows two of the matched channels. It can be observed from Figure 3.10 that PVC has a higher thermal resistance than the MDMO-PPV layer.

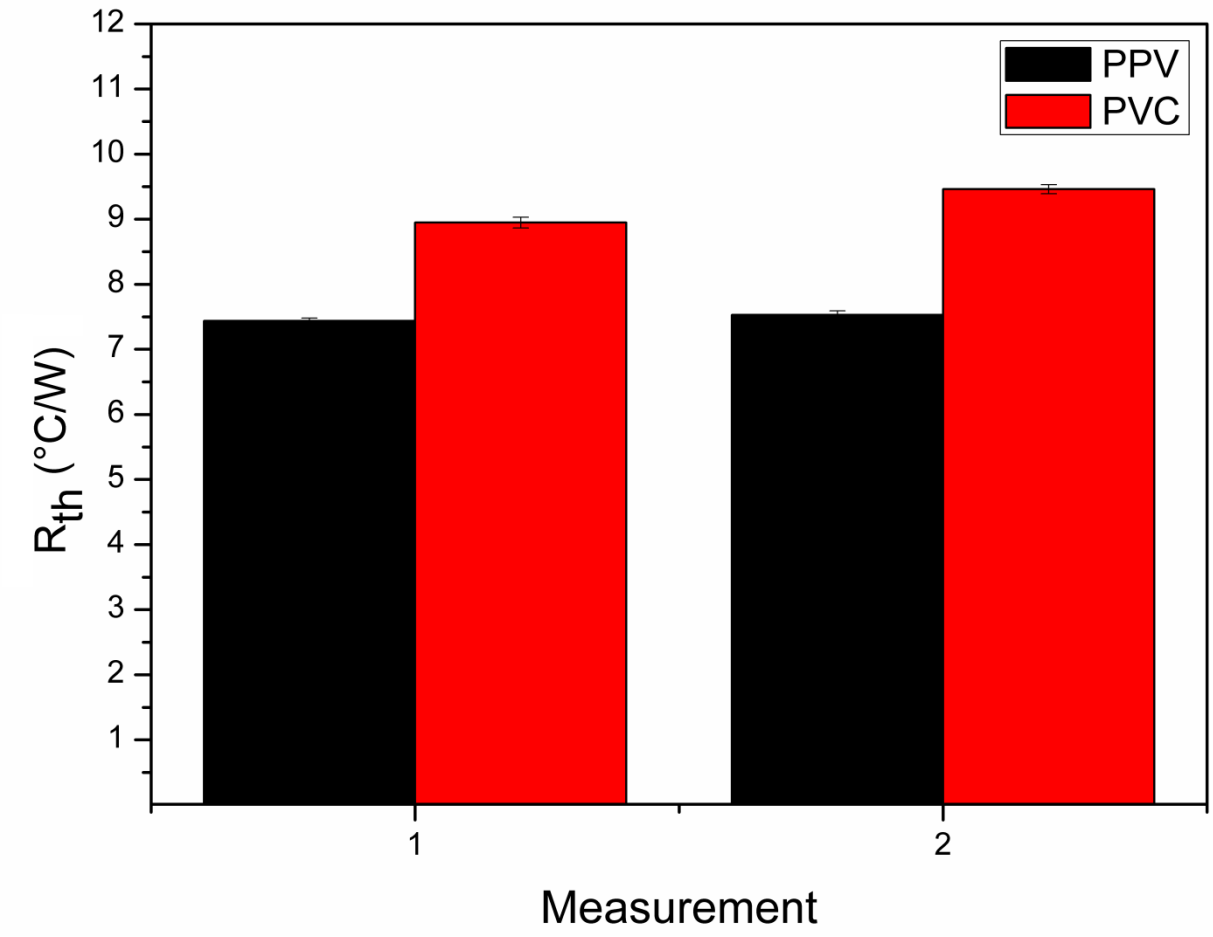


**Figure 3.10,** Absolute $R_{th}$ of PVC and MDMO-PPV**.**

# Chapter 4: Conclusion

The heat-transfer method has been successfully adapted to an array format using the new flow cell design with four segmented cavities. The quadrant separation, limit of detection, specificity and cross selectivity proved to be adequate along with a reduced volume of the cavities which is beneficial for biological samples which are often low in volume.

By means of microscopy analysis it was demonstrated that it is possible to functionalize a substrate with multiple different MIPs or NIPs in order to create an array. This lack of interference allows a low level of intra-sample variability for the MIP sensor. The dose response curve of a single quadrant functionalized with L-nicotine MIPs resulted in a limit of detection which is approximately the same as was found with the previous setup.

Experiments in which three identical MIPs were used for the functionalization of a single substrate showed nearly identical responses between all channels. Due to the nearly identical effect size of all three channels, it is possible to create arrays which utilize multiple separate channels allowing high throughput applications.

Analogous to the experiment with three equal MIPs, a substrate was prepared with three different MIPS for the target molecules serotonin, histamine and L-nicotine. All three MIPs were placed on different segments along with a NIP on the fourth segment. After adding the respective target molecules to the MIP, all three channels showed a nearly identical response to their target. The similar response between different MIPs is important for making and array containing multiple different MIPs targeted towards different molecules.

Functionalization with MIPs for different targets demonstrated the possibility of array formats for MIPs. Therefore two arrays were created which are able to distinguish between histamine and serotonin or between L-nicotine and serotonin. A significant response was only seen when the target molecules came into contact with their respective MIP. Non-target MIPs evoked no significant change in $R_{th}$ in all channels. The first array containing histamine and L-nicotine proved to be successful in discriminating between a histamine solution and L-nicotine solution with no significant response to non-target molecules. The second array which was functionalized with histamine and serotonin also proved to be capable of distinguishing between both solutions without response to non-target molecules. This proves that even though the targets are chemically similar, the MIPs will only show a change in thermal resistance upon exposure to their corresponding target without cross selectivity.

The novel heat-transfer method in combination with the miniaturized, array format flow cell makes it possible to measure the concentration of different target molecules up to the nanomolar range. Discrimination between similar small organic molecules was possible, showing no significant cross selectivity.

An improvement could lie in the application of the MIPs and NIPs to the substrate, preliminary results with spray-coating as a method of application showed promising results. Further optimization of the new array formatted flow cell can be found in the manual insertion and adjustment of the thermocouples. Fixating the thermocouples to the flow cell would reduce the chance of movement

during measurements, however the current design does not allow for this modification and a new flow cell with fixed thermocouples is currently being designed.

The capillary whole blood flow cell demonstrated a first experimental application where the heat-transfer method, MIPs in array format and correction for non-specific binding were combined into a working device. However the concentrations used in the experiments are higher than found in normal human blood and therefore these experiments should be seen as proof of principle experiments.

The increased throughput that was gained with the array formatted flow cell improves the potential of MIP based biosensors for future bioanalytical applications. Correction for non-specific binding within the array increases accuracy of the measurements due to a lower variance between sensors. However the biggest gain was found in the capability to discriminate between multiple small organic molecules with a single sensor substrate. The ability to detect and distinguish between small organic molecules is useful for various applications ranging from medical to environmental analysis. Combined with the already proven high speed, low-cost and high specificity there is a great potential for clinical and commercial applications.

# References


1. Herrero-Hernández E, Carabias-Martínez R, Rodríguez-Gonzalo E. Use of a bisphenol-A imprinted polymer as a selective sorbent for the determination of phenols and phenoxyacids in honey by liquid chromatography with diode array and tandem mass spectrometric detection. Anal Chim Acta. 2009 Sep 21;650(2):195–201.

2. Jenik M, Seifner A, Lieberzeit P, Dickert FL. Pollen-imprinted polyurethanes for QCM allergen sensors. Anal Bioanal Chem. 2009 May;394(2):523–8.

3. Bers K, van Grinsven B, Vandenryt T, Murib M, Janssen W, Geerets B, et al. Implementing heat transfer resistivity as a key element in a nanocrystalline diamond based single nucleotide polymorphism detection array. Diam Relat Mater. 2013 Sep;38:45–51.

4. Ruela ALM, Figueiredo EC, Pereira GR. Molecularly imprinted polymers as nicotine transdermal delivery systems. Chem Eng J. 2014;

5. Kotova K, Hussain M, Mustafa G, Lieberzeit PA. MIP sensors on the way to biotech applications: Targeting selectivity. Sensors Actuators B Chem. 2013 Dec;189:199–202.

6. Mosbach K. Molecular imprinting. Trends Biochem Sci. 1994 Jan;19(1):9–14.

7. Shimizu KD, Stephenson CJ. Molecularly imprinted polymer sensor arrays. Curr Opin Chem Biol. 2010 Dec;14(6):743–50.

8. Contin M, Flor S, Martinefski M, Lucangioli S, Tripodi V. The use of coenzyme Q0 as a template in the development of a molecularly imprinted polymer for the selective recognition of coenzyme Q10. Anal Chim Acta. 2014 Jan 7;807:67–74.

9. Gültekin A, Karanfil G, Kuş M, Sönmezoğlu S, Say R. Preparation of MIP-based QCM nanosensor for detection of caffeic acid. Talanta. 2014 Feb 15;119:533–7.

10. Yang Z, Zhang C. Designing of MIP-based QCM sensor for the determination of Cu(II) ions in solution. Sensors Actuators B Chem. 2009 Oct;142(1):210–5.

11. Peeters M, Troost FJ, van Grinsven B, Horemans F, Alenus J, Murib MS, et al. MIP-based biomimetic sensor for the electronic detection of serotonin in human blood plasma. Sensors Actuators B Chem. 2012 Aug;171-172:602–10.

12. Eersels K, van Grinsven B, Ethirajan A, Timmermans S, Jiménez Monroy KL, Bogie JFJ, et al. Selective Identification of Macrophages and Cancer Cells Based on Thermal Transport through Surface-Imprinted Polymer Layers. ACS Appl Mater Interfaces. American Chemical Society; 2013 Jul 2;5(15):7258–67.

13. Karim K, Breton F, Rouillon R, Piletska E V, Guerreiro A, Chianella I, et al. How to find effective functional monomers for effective molecularly imprinted polymers? Adv Drug Deliv Rev. 2005 Dec 6;57(12):1795–808.

14. Owens PK, Karlsson L, Lutz ESM, Andersson LI. Molecular imprinting for bio- and pharmaceutical analysis. TrAC - Trends in Analytical Chemistry. 1999. p. 146–54.

15. Sellergren B, Allender CJ. Molecularly imprinted polymers: a bridge to advanced drug delivery. Adv Drug Deliv Rev. 2005 Dec 6;57(12):1733–41.

16. Spivak D a. Optimization, evaluation, and characterization of molecularly imprinted polymers. Adv Drug Deliv Rev. 2005 Dec 6;57(12):1779–94.

# References


17. Shalon D, Smith SJ, Brown PO. A DNA microarray system for analyzing complex DNA samples using two-color fluorescent probe hybridization. Genome Res. 1996 Jul 1;6(7):639–45.

18. Greene NT, Morgan SL, Shimizu KD. Molecularly imprinted polymer sensor arrays. Chem Commun. The Royal Society of Chemistry; 2004;(10):1172–3.

19. Takeuchi T, Goto D, Shinmori H. Protein profiling by protein imprinted polymer array. Analyst. The Royal Society of Chemistry; 2007;132(2):101–3.

20. Hawari HF, Samsudin NM, Shakaff AYM, Wahab Y, Hashim U, Zakaria A, et al. Highly selective molecular imprinted polymer (MIP) based sensor array using interdigitated electrode (IDE) platform for detection of mango ripeness. Sensors Actuators B Chem. 2013 Oct;187:434–44.

21. Alenus J, Ethirajan a, Horemans F, Weustenraed a, Csipai P, Gruber J, et al. Molecularly imprinted polymers as synthetic receptors for the QCM-D-based detection of L-nicotine in diluted saliva and urine samples. Anal Bioanal Chem. 2013 Aug;405(20):6479–87.

22. Bers K, Eersels K, van Grinsven B, Daemen M, Bogie JFJ, Hendriks JJ a, et al. Heat-Transfer Resistance Measurement Method (HTM)-Based Cell Detection at Trace Levels Using a Progressive Enrichment Approach with Highly Selective Cell-Binding Surface Imprints. Langmuir. 2014 Mar 19;

23. Gershon MD, Tack J. The serotonin signaling system: from basic understanding to drug development for functional GI disorders. Gastroenterology. 2007 Jan;132(1):397–414.

24. Kettell J, Jones R, Lydeard S. Reasons for consultation in irritable bowel syndrome: symptoms and patient characteristics. Br J Gen Pract. 1992 Nov;42(364):459–61.

25. Drossman DA, Li Z, Andruzzi E, Temple RD, Talley NJ, Grant Thompson W, et al. U. S. Householder survey of functional gastrointestinal disorders - Prevalence, sociodemography, and health impact. Dig Dis Sci. 1993;38:1569–80.

26. Everhart JE, Renault PF. Irritable bowel syndrome in office-based practice in the United States. Gastroenterology. 1991;100:998–1005.

27. Sandler RS, Jordan MC, Shelton BJ. Demographic and dietary determinants of constipation in the US population. Am J Public Health. American Public Health Association; 1990 Feb 1;80(2):185–9.

28. Levy RL, Korff M, Whitehead WE, Stang P, Saunders K, Jhingran P, et al. Costs of care for irritable bowel syndrome patients in a health maintenance organization. Am J Gastroenterol. The American College of Gastroenterology; 2001 Nov;96(11):3122–9.

29. Sandler RS, Everhart JE, Donowitz M, Adams E, Cronin K, Goodman C, et al. The burden of selected digestive diseases in the United States. Gastroenterology. 2002 May;122(5):1500–11.

30. Gralnek IM, Hays RD, Kilbourne A, Naliboff B, Mayer EA. The impact of irritable bowel syndrome on health-related quality of life. Gastroenterology. 2000 Sep;119(3):654–60.

31. Keszthelyi D, Troost FJ, Masclee AAM. Understanding the role of tryptophan and serotonin metabolism in gastrointestinal function. Neurogastroenterol Motil. Blackwell Publishing Ltd; 2009 Dec 1;21(12):1239–49.

32. Lesurtel M, Soll C, Graf R, Clavien P. Role of serotonin in the hepato-gastroIntestinal tract: an old molecule for new perspectives. Cell Mol Life Sci. 2008 Mar;65(6):940–52.

# References


33. Barbara G, Stanghellini V, De Giorgio R, Cremon C, Cottrell GS, Santini D, et al. Activated mast cells in proximity to colonic nerves correlate with abdominal pain in irritable bowel syndrome. Gastroenterology. 2004 Mar;126(3):693–702.

34. Yoshitake T, Ichinose F, Yoshida H, Todoroki K, Kehr J, Inoue O, et al. A sensitive and selective determination method of histamine by HPLC with intramolecular excimer-forming derivatization and fluorescence detection. Biomed Chromatogr. John Wiley & Sons, Ltd.; 2003 Dec 1;17(8):509–16.

35. Keyzer JJ, Wolthers BG, Muskiet FAJ, Breukelman H, Kauffman HF, de Vries K. Measurement of plasma histamine by stable isotope dilution gas chromatography-mass spectrometry: Methodology and normal values. Anal Biochem. 1984 Jun;139(2):474–81.

36. Ujike a, Ishikawa Y, Ono M, Yuasa T, Yoshino T, Fukumoto M, et al. Modulation of immunoglobulin (Ig)E-mediated systemic anaphylaxis by low-affinity Fc receptors for IgG. J Exp Med. 1999 May 17;189(10):1573–9.

37. Athikomrattanakul U, Gajovic-Eichelmann N, Scheller FW. Thermometric Sensing of Nitrofurantoin by Noncovalently Imprinted Polymers Containing Two Complementary Functional Monomers. Anal Chem. American Chemical Society; 2011 Sep 29;83(20):7704–11.

38. Louwet F, Vanderzande D, Gelan J. A general synthetic route to high molecular weight poly(p-xylylene)-derivatives: a new route to poly(p-phenylene vinylene). Synth Met. 1995 Mar;69(1-3):509–10.

39. Peeters M, Troost FJ, Mingels RHG, Welsch T, van Grinsven B, Vranken T, et al. Impedimetric Detection of Histamine in Bowel Fluids Using Synthetic Receptors with pH-Optimized Binding Characteristics. Anal Chem. American Chemical Society; 2012 Dec;85(3):1475–83.

40. Thoelen R, Vansweevelt R, Duchateau J, Horemans F, D'Haen J, Lutsen L, et al. A MIP-based impedimetric sensor for the detection of low-MW molecules. Biosens Bioelectron. 2008 Jan;23(6):913–8.

41. Geerets B, Peeters M, Grinsven B. Optimizing the Thermal Read-Out Technique for MIP-Based Biomimetic Sensors: Towards Nanomolar Detection Limits. Sensors. 2013;1–12.

# References

# Supplemental Information

Articles authored and co-authored:

*Sensors* **2014**, *14*, 1-x manuscripts; doi:10.3390/s140x0000x

OPEN ACCESS

*sensors*

ISSN 1424-8220

www.mdpi.com/journal/sensors

*Communication*

## Array formatting of the heat-transfer method (HTM) for the detection of small organic molecules by molecularly imprinted polymers

G. Wackers[1,†], T. Vandenryt[1,†], P. Cornelis[1], E. Kellens[1,2], R. Thoelen[1,2], W. De Ceuninck[1,2,*], P. Losada-Pérez[1,2], B. van Grinsven[1,2,3], M. Peeters[1,2], and P. Wagner[1,2]

[1] Hasselt University, Institute for Materials Research, Wetenschapspark 1, B-3590 Diepenbeek, Belgium

[2] IMEC vzw – Division IMOMEC, Wetenschapspark 1, B-3590 Diepenbeek, Belgium

[3] Maastricht Science Programme, Maastricht University, 6200 MD Maastricht, Netherlands

[†] Authors contributed equally to this work

* Author to whom correspondence should be addressed; E-Mail: Ward.Deceuninck@uhasselt.be; Tel.: +32-11268872; Fax: +32-11268899

*Received: / Accepted: / Published:*

**Abstract:** In this work we present the first steps towards a molecularly imprinted polymer (MIP) based biomimetic sensor array for the detection of small organic molecules via the heat-transfer method (HTM). HTM relies on the change in thermal resistance upon binding of the target molecule to the MIP-type receptor. A flow-through sensor cell was developed, which is segmented into four quadrants with a volume of 2.5 µL each, allowing four measurements to be done simultaneously on a single substrate. Verification measurements were conducted, in which all quadrants received a uniform treatment and all four channels exhibited a similar response. Subsequently, measurements were performed in quadrants, which were functionalized with different MIP particles. Each of these quadrants was exposed to the same buffer solution, spiked with different molecules, according to the MIP under analysis. With the flow cell design we could discriminate between similar small organic molecules and observed no significant cross-selectivity. Therefore, the MIP array sensor platform with HTM as a readout technique, has the potential to become a low-cost analysis tool for bioanalytical applications.

**Keywords:** heat-transfer method (HTM); molecularly imprinted polymers (MIPs); serotonin; histamine; L-nicotine, array format.

# Heat transfer resistance as a tool to quantify hybridization efficiency of DNA on a nanocrystalline diamond surface.

P. Cornelis[1,†], T. Vandenryt[1,2,†], G. Wackers[1], E. Kellens[1,3], P. Losada-Pérez[1], R. Thoelen[1,3], W. De Ceuninck[1,3], K. Eersels[1,*], S. Drijkoningen[1], K. Haenen[1], M. Peeters[1,3], B. van Grinsven[1,4], P. Wagner[1,3]

[1] Hasselt University, Institute for Materials Research, Wetenschapspark 1, B-3590 Diepenbeek, Belgium
[2] XIOS University College, Department of Applied Engineering, Agoralaan – Building H, B-3590 Diepenbeek, Belgium
[3] IMOMEC, Wetenschapspark 1, B-3590 Diepenbeek, Belgium
[4] Maastricht Science Programme, Maastricht University, Post Office Box 616, 6200 MD Maastricht, Netherlands

[†] Authors contributed equally to this work

[*] Author to whom correspondence should be addressed; E-Mail: Kasper.Eersels@uhasselt.be; Tel.: +32-11-26-88xx; Fax: +32-11-26-8813

**Abstract**

In this article, we report on a label-free real-time method based on heat transfer resistivity for thermal monitoring of DNA denaturation and its potential to quantify DNA fragments with a specific sequence of interest. Probe DNA, consisting of a 36-mer fragment was covalently immobilized on a nanocrystalline diamond surface, created by chemical vapor deposition on a silicon substrate. Various concentrations of full matched 29-mer target DNA fragments were hybridized with this probe DNA. We observed that the change in heat transfer resistance upon denaturation depends on the concentration of target DNA used during the hybridization, which allowed to determine the dose response curve. Therefore, these results illustrate the potential of this technique to quantify the concentration of a specific DNA fragment and to quantify the hybridization efficiency to its probe.

Supplemental information

# Auteursrechtelijke overeenkomst

Ik/wij verlenen het wereldwijde auteursrecht voor de ingediende eindverhandeling:
**Array formatting of the heat-transfer method (HTM) for the detection of small organic molecules by molecularly imprinted polymers**

Richting: **master in de biomedische wetenschappen-bio-elektronica en nanotechnologie**
Jaar: **2014**

in alle mogelijke mediaformaten, - bestaande en in de toekomst te ontwikkelen - , aan de Universiteit Hasselt.

Niet tegenstaand deze toekenning van het auteursrecht aan de Universiteit Hasselt behoud ik als auteur het recht om de eindverhandeling, - in zijn geheel of gedeeltelijk -, vrij te reproduceren, (her)publiceren of distribueren zonder de toelating te moeten verkrijgen van de Universiteit Hasselt.

Ik bevestig dat de eindverhandeling mijn origineel werk is, en dat ik het recht heb om de rechten te verlenen die in deze overeenkomst worden beschreven. Ik verklaar tevens dat de eindverhandeling, naar mijn weten, het auteursrecht van anderen niet overtreedt.

Ik verklaar tevens dat ik voor het materiaal in de eindverhandeling dat beschermd wordt door het auteursrecht, de nodige toelatingen heb verkregen zodat ik deze ook aan de Universiteit Hasselt kan overdragen en dat dit duidelijk in de tekst en inhoud van de eindverhandeling werd genotificeerd.

Universiteit Hasselt zal mij als auteur(s) van de eindverhandeling identificeren en zal geen wijzigingen aanbrengen aan de eindverhandeling, uitgezonderd deze toegelaten door deze overeenkomst.

Voor akkoord,

**Wackers, Gideon**

Datum: **10/06/2014**